ELSEVIER

Polymer 43 (2002) 823–829

polymer

www.elsevier.com/locate/polymer

A study of blending and complexation of poly(acrylic acid)/poly(vinyl pyrrolidone)

Cheryl Lau, Yongli Mi*

Department of Chemical Engineering, The Hong Kong University of Science and Technology, Clear Water Bay, Kowloon, Hong Kong, People's Republic of China

Received 22 May 2001; received in revised form 2 September 2001; accepted 10 September 2001

Abstract

Poly(acrylic acid) (PAA) and poly(vinyl pyrrolidone) (PVP) were chosen to prepare polymer complex and blends. The complex was prepared from ethanol solution and the blends were prepared from 1-methyl-2-pyrrolidone solution. DSC results show that the T_gs of the PAA/PVP blends lie between those of the two constituent polymers, whereas T_g of the PAA/PVP complex is higher than both blends and the two constituent polymers. TGA results show that degradation temperature, T_d, of PAA increases upon adding PVP in the blend, but thermal stability of the complex is higher than that of the blends as reflected by the higher T_d. Both FTIR and high-resolution solid state NMR show strong hydrogen bonding between PAA and PVP by showing significant chemical shift. The $T_{1\rho}$(H) measurement shows that the homogeneity scale for the blend is at ~20 Å and that for the complex is ~15 Å.

Keywords: Poly(acrylic acid) and poly(vinyl pyrrolidone); Complex; Blends

1. Introduction

Formation of interpolymer complexes can be achieved through the specific interactions such as electrostatic interactions, hydrogen bonding, and hydrophobic interactions, etc. [1,2]. The interpolymer complexes resulting from these interactions possess distinguished characteristics that are different from those of the individual components [3,4]. For polymer blends, the combinatorial entropy of mixing is negligibly small and the free volume contribution further increases the free energy of mixing. As a result, the miscibility depends either on specific interactions or on intramolecular repulsion. Various types of specific interactions are responsible for miscibility, such as hydrogen bonding, dipolar interactions, charge transfer complex formation, ion interactions, Lewis acid–base interactions, phenyl group coupling etc. All these contribute to the negative heat of mixing [5]. By comparing the domain size and segmental miscibility of polymer complexes and blends and by studying the controlled complexation process, one can learn how to design the useful engineering materials for special applications.

In this study, polymer complex and blends of Poly(acrylic acid) (PAA) and poly(vinyl pyrrolidone) (PVP) were prepared. PVP is a biocompatible material and both PAA and PVP have wide applications as biomaterials. The PAA/PVP complex was prepared from ethanol and the blends were prepared from 1-methyl-2-pyrrolidone (NMP) solution. The experimental techniques employed in this study are differential scanning calorimetry (DSC), thermogravimetric analysis (TGA), X-ray photoelectron spectroscopy, Fourier transform infrared spectroscopy (FTIR), and high-resolution ^{13}C solid-state nuclear magnetic resonance spectroscopy (NMR).

2. Experimental

2.1. Materials and samples preparation

PAA used in this study was purchased from Aldrich Chemical Company, Inc., USA and it has a quoted molecular weight of viscosity (M_v) of 450,000 and T_g of 106°C. PVP with a number-average molecular weight (M_n) of 360,000 was obtained from Scientific Polymer Products, Inc., USA. PAA/PVP complex was prepared by dissolving pure PAA and pure PVP separately in ethanol. Each solution was stirred overnight to ensure complete dissolution. The two solutions were then mixed together in a molar ratio of 1:1 to give a white precipitate. The precipitate was filtered and washed with ethanol. The samples were then dried under

* Corresponding author. Fax: +852-358-0054.
E-mail address: keymix@usthk.ust.hk (Y. Mi).

0032-3861/02/$ - see front matter
PII: S0032-3861(01)00641-3

Table 1
PAA/PVP blends composition

PAA/PVP blends	wt/wt	mol/mol
	60/40	2/1
	40/60	1/1
	22/78	1/2

vacuum at 40°C for 6 weeks to remove all the residue solvent. PAA/PVP blends were prepared with three different compositions as listed in Table 1. Films of pure polymers and their blends were prepared by solution casting using NMP as a common solvent. PAA was dissolved in the solvent with continuous heating and stirring. After all PAA was dissolved in the NMP, an appropriate amount of PVP was added and the solution was heated with stirring until all the samples dissolved. After all the samples dissolved, the solution obtained was clear and yellow in color. The majority of the solvent was removed at 100°C in an oven for a week. To further remove the residual solvent, all the blend films were dried under vacuum at 100°C for 6 weeks.

Thin films of samples for FTIR analysis were prepared by casting the NMP solutions onto NaCl plates. The films were dried at 100°C in a regular oven followed by a vacuum oven for 2 weeks. All films used in this study were sufficiently thin to be within the absorbance range where the Lambert–Beer law is obeyed.

2.2. Techniques

2.2.1. X-ray photoelectron spectroscopy

The model used was PHI 5600 (Physical electronics). Aluminum anode was used as the X-ray source. The pass energy values taken were 23.5 and 187.85 eV. The acquisition time was ranged from 10 to 40 min.

2.2.2. Differential scanning calorimetry

The calorimetric measurements were conducted on a TA 2910 differential scanning calorimeter in dry nitrogen atmosphere. The instrument was calibrated with indium and zinc standards. For all the blends and complex, the samples were first scanned from 25 to 250°C at 20°C/min, followed by quenching to 25°C and then scanned to 250°C at 20°C/min. The values of T_g were taken as the midpoint of the heat capacity transition.

2.2.3. Thermogravimetric analysis

The thermal stability measurements were conducted by a TA 2950 thermogravimetric analyzer in dry nitrogen atmosphere. All the blends and the complex were heated at 10°C/min from 25 to 600°C. The temperature at which an abrupt decrease in sample weight occurred was designated as the decomposition temperature, T_d.

2.2.4. Fourier transform infrared spectroscopy

Infrared spectra of the system were recorded on a Bomem MB104 Fourier transform infrared spectrometer for the investigation of intermolecular interactions. All the spectra were obtained at room temperature with a resolution of 2 cm^{-1} and were signal averaged over 64 scans.

2.2.5. High-resolution ^{13}C solid state NMR spectroscopy

The rate of magic angle spinning was 5.0–5.8 kHz for measuring ^{13}C spectra and relaxation times. The cross polarization (CP) Hartmann–Hahn contact time was varied from 1.5–2.0 ms to observe the spectra of the pure components, their blends and complex. 512 scans were used for the signal accumulation in obtaining the ^{13}C spectra and 400 scans were used for relaxation time measurements. In all experiments, a recycle delay of 10 s was used in order for the net magnetization to be completely relaxed.

3. Results and discussion

3.1. Characterization of Complex

3.1.1. X-ray photoelectron spectroscopy

The atomic mass of the repeat unit of PAA and PVP is 72 and 111, respectively. The extent of complexation was analyzed for PAA/PVP complex and was calculated for the carbon and nitrogen content obtained from the elemental analysis. The results are presented in Table 2. It is seen that although the sample was complexed in a molar ratio of 1:1, the PVP/PAA ratio in the complex is 1.5:1.

3.2. Thermal analysis

3.2.1. Differential scanning calorimetry

All the PAA/PVP blend films cast from NMP were transparent at room temperature, suggesting that no phase separation occurred in the blends on the scale exceeding the wavelength of the visible light. On the contrary, white solid is obtained for the complex. The glass transition temperatures of PAA and PVP are 106 and 184°C, respectively from

Table 2
Elemental analysis for PAA/PVP complex

Atomic concentration		Composition in preparation		Composition in products	
C (%)	N (%)	wt/wt	mol/mol	wt/wt	mol/mol
70.20	6.73	40/60	1/1	49/51	1.48/1

Table 3
Decomposition temperature (T_d) and glass transition temperature (T_g) of PAA, PVP, their blends, and complex from TGA and DSC measurements

	Sample	wt/wt	mol/mol	T_d (°C)	T_g (°C)
	PAA	100/0		203	106
PAA/PVP	Blend	60/40	2/1	210	166
PAA/PVP	Blend	40/60	1/1	221	174
PAA/PVP	Blend	22/78	1/2	222	163
	PVP	0/100		400	184
PAA/PVP	Complex	49/51	1/1	261	205

the DSC measurements. The glass transition temperature of the blends and the complexes are also obtained and summarized in Table 3. The T_g composition curve for the blends is shown in Fig. 1. Both blends and complex exhibit single T_g. For miscible blends, T_g can be described by several empirical equations [6–9] and the Kwei equation is usually employed for systems with specific interactions,

$$T_g = \frac{W_1 T_{g1} + kW_2 T_{g2}}{(W_1 + kW_2)} + qW_1 W_2 \quad (1)$$

where T_g is the glass transition temperature of the blend; T_{g1} and T_{g2} are those of the pure components; W_1 and W_2 are the weight fractions of the two components; k and q are adjustable parameters. The application of Eq. (1) on the T_g-composition data of the PAA/PVP blends was best fitted by a S-shaped curve (Fig. 1) with $k = 0.08$ and $q = 240$. It is found that the T_gs of the blends lie between those of the two pure components, but the T_g of the PAA/PVP complex (205°C) is significantly higher than those of the blends and the two pure components. The appearance of the single T_g for the PAA/PVP blends and complex indicates that they exhibit a miscible homogeneous amorphous phase.

3.2.2. Thermogravimetric analysis

The TGA thermograms of PAA, PVP, and their blends and complex are shown in Fig. 2. The TGA results are summarized in Table 3. It is observed that the PAA has much lower thermal stability than PVP. Therefore, the thermal stability of the blends is generally poor and close to the PAA end. The T_d of the blends increases with the increase in the PVP content. However, it is interesting to note that T_d of the complex is higher than those of the blends at any composition. This indicates that hydrogen bonding between PAA and PVP can stabilize PAA. In the case of the complex, since the chains are more closely tangled together, the decomposition temperature of the complex is even higher than that of the blends. This suggests that the more intimate mixing and stronger interaction between polymers will increase the thermal stability.

3.3. Spectroscopic analysis

3.3.1. Fourier transform infrared spectroscopy

FTIR is one of the most powerful tools to detect hydrogen bonding in polymers. The infrared spectrum of pure PAA is shown in Fig. 3. It has been reported that atactic PAA has a characteristic absorption at 1250 cm^{-1} with a weak shoulder at 1300 cm^{-1} while syndiotactic PAA gives an absorption

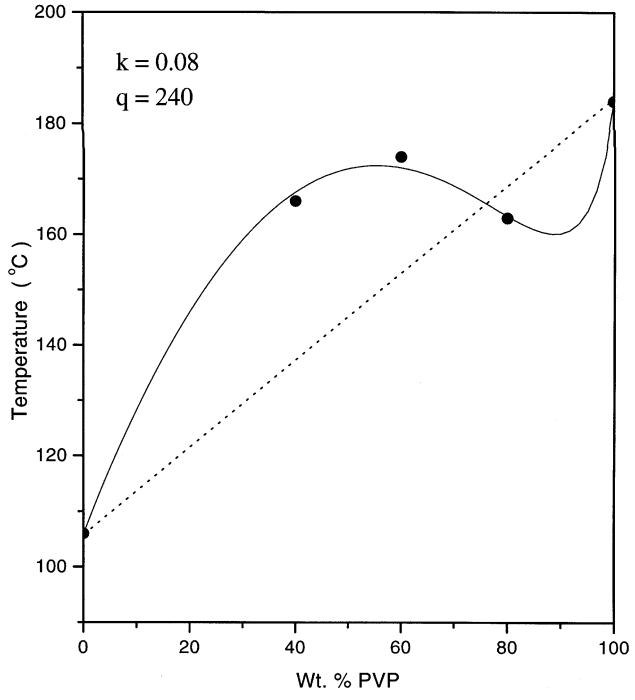

Fig. 1. Plot of T_g versus the composition of PAA/PVP blends. The S-shaped curve is calculated using the Kwei equation with $k = 0.08$ and $q = 240$.

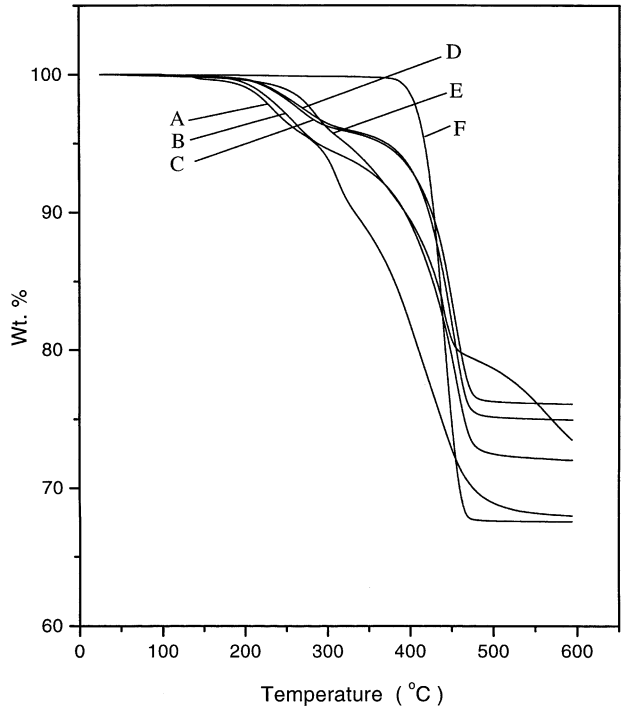

Fig. 2. TGA thermograms of the PAA/PVP blends and the complex: (A) 0; (B) 40; (C) 60; (D) 78; (E) PAA/PVP complex (1/1); (F) 100 wt% PVP.

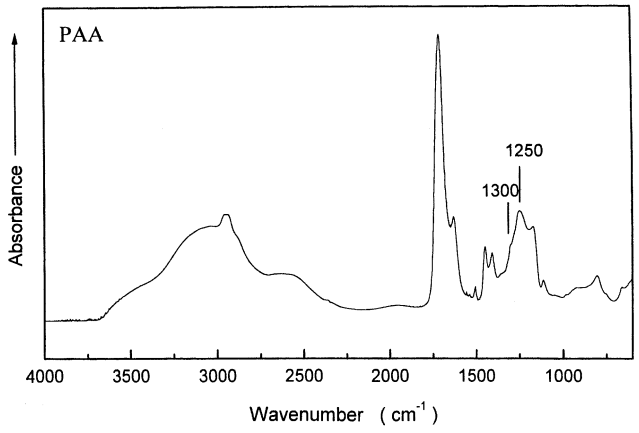

Fig. 3. FTIR spectrum of PAA.

band at 1240 cm^{-1} [7]. The absorption band at 1250 cm^{-1} and the shoulder at 1300 cm^{-1} in Fig. 3 indicate that the PAA used in this study is atactic.

The FTIR spectra in the carbonyl stretching region for the PAA/PVP blends are shown in Fig. 4. For pure PVP, the absorption band at 1660 cm^{-1} is called amide-I and is a combined mode with the contribution of >C=O and C–N stretch [8]. Owing to this combination mode, this band occurred at a lower wave number than expected for pure

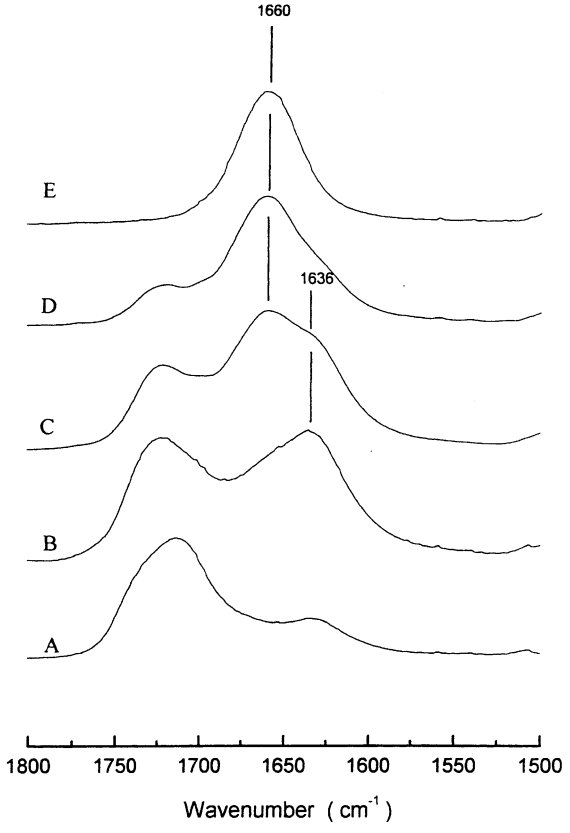

Fig. 4. FTIR spectra in the carbonyl region of the PAA/PVP blends: (A) 0; (B) 40; (C) 60; (D) 78; (E) 100 wt% PVP.

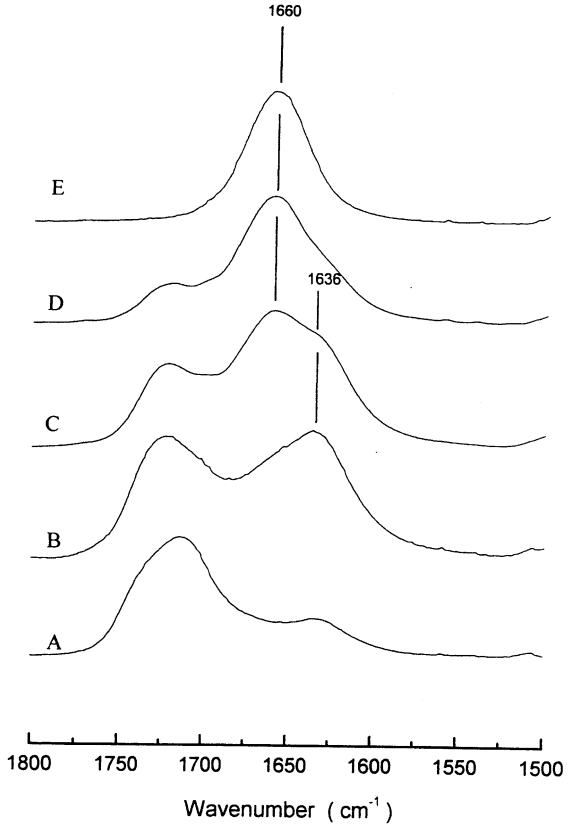

Fig. 5. ^{13}C CP/MAS/DD spectra of the PAA/PVP blends: (A) 0; (B) 40; (C) 60; (D) 78; (E) PAA/PVP complex (1/1); (F) 100 wt% PVP.

ester carbonyl band (1750–1700 cm^{-1}). In this study, we will refer this band as the carbonyl band of PVP. The spectra of the blends display absorption bands at frequencies that represent the characteristic absorption bands of the component polymers. An addition of 20 wt% PAA in PVP did not have significant change in the spectra. By increasing PAA content, a new band at around 1636 cm^{-1} appeared which is attributed to the hydrogen-bonded carbonyl group of PVP in which the hydrogen bonds are formed with the hydroxyl group of PAA. The intensity of this band increases upon increasing PAA content in the blends. Since the PVP carbonyl group is hydrogen bonded to the PAA hydroxyl group, the absorption band shifts to the lower wave numbers, as can be observed in spectra B and C of Fig. 4.

Moreover, the chemical shift, $\Delta\nu = 24$ cm^{-1}, indicates that the hydrogen bonding is rather strong. This supports the DSC results that the T_g composition curve exhibits an S-shape that is common for strong hydrogen bond blends.

3.3.2. ^{13}C CP/MAS/DD solid state NMR spectra

In order to ascertain the miscibility of PAA/PVP blends at the molecular level, high-resolution ^{13}C solid state NMR was applied to study the miscibility scale of these systems. ^{13}C CP/MAS/DD spectra of PAA, PVP, their blends, and complex are shown in Fig. 5. Although it has three carbons

Table 4
Assignment of ^{13}C CP/MAS/DD solid state NMR spectra for PAA and PVP

Polymer	δ (ppm)	Assignment
PAA	183	–C(3)OOH
	40–30	–C(2)H and –C(1)H_2–
PVP	176	–C(6)=O
	44	–C(2)H– and –C(3)H_2–
	38	–C(1)H_2–
	33	–C(5)H_2–
	19	–C(4)H_2–

in its structure, only two resonance lines are observed for pure PAA. The broad band at 40–30 ppm is assigned to the α and β carbon [10]. Similarly for pure PVP, there are some overlaps of resonance carbons, only four resonance lines can be resolved in the spectra although PVP has six carbons. Since both C(2)H and C(3)H_2 of PVP are attached to the nitrogen atom, they experience similar chemical environment and hence they have the same chemical shift. The difference between the resonance line at 38 ppm for C(1)H_2 and that at 33 ppm for C(5)H_2 are seen as one broad peak instead of two due to overlapping. The peak assignment is illustrated in Fig. 5 and Table 4.

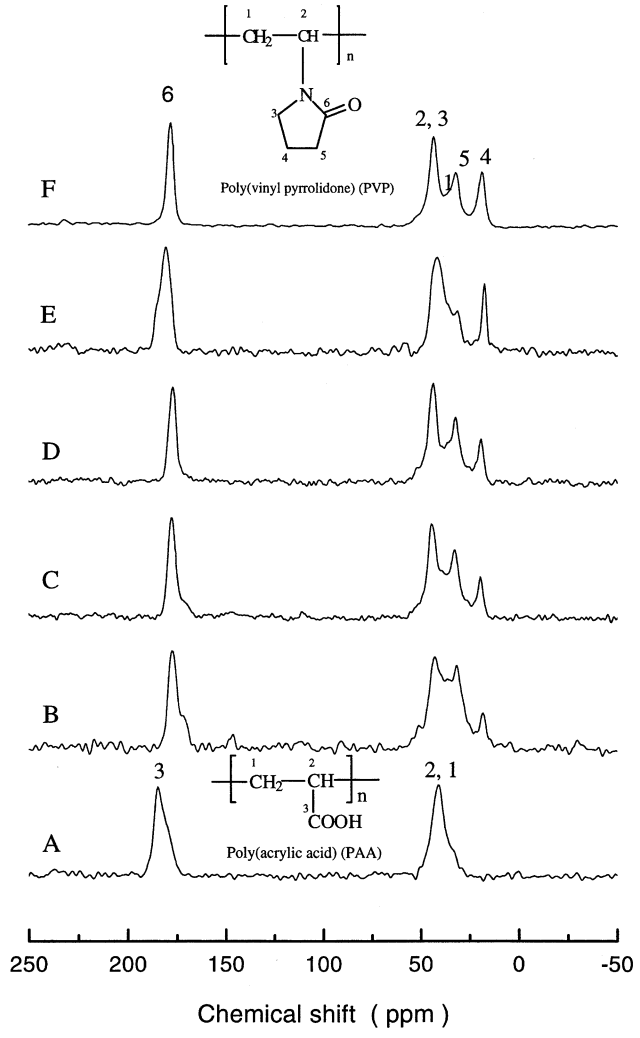

Fig. 6. Plot of chemical shift of carbonyl peak versus composition.

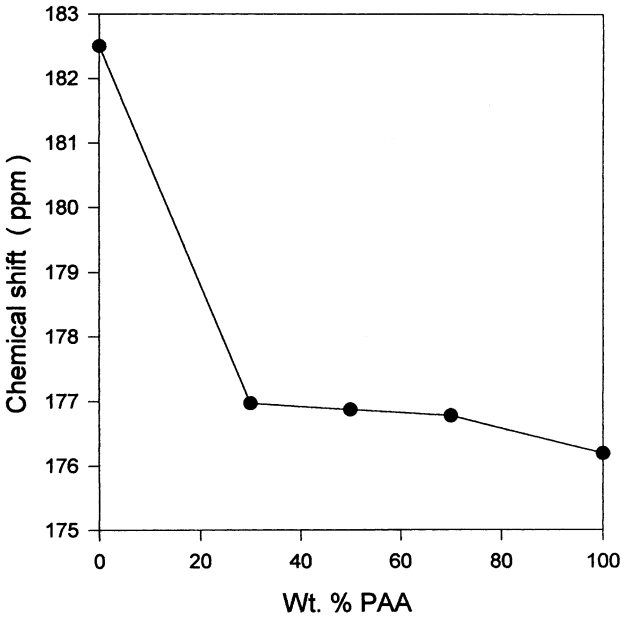

Fig. 7. ^{13}C CP/MAS/DD spectra in the carbonyl region of the PAA/PVP blends: (A) 0; (B) 40; (C) 60; (D) 78; (E) PAA/PVP complex (1/1); (F) 100 wt% PVP.

It is accepted that the ^{13}C chemical shift of polymers observed in high-resolution ^{13}C NMR spectra in solution is sensitive to their microstructures, i.e. stereoregularity, comonomer sequence, and defect structures [11]. Recently, it has been demonstrated that the microstructural sensitivity of polymer chemical shifts has its origin in local chain conformation [12]. Microstructural difference induces changes in local chain conformation that in turn are manifested in ^{13}C chemical shifts for the carbon atoms in the vicinity of each unique microstructure [9,10,13–15]. PAA has a carbonyl carbon resonance at 183 ppm while PVP at 176 ppm. From the spectra of the blends and the complex, one can observe that only one resonance peak of the carbonyl carbon can be found at around 177 ppm for the blends and at 179 ppm for the complex. Fig. 6 shows the change in chemical shift with blend composition. Fig. 7 shows the shift of the carbonyl carbon resonance in the ^{13}C NMR spectra.

3.3.3. Proton spin–lattice relaxation times

In homogenous system, the protons of different chemical chains can be closely coupled and relax at an identical rate through spin-diffusion mechanism, while protons in heterogeneous system relax at an independent rate. Therefore, the NMR criteria for miscibility are that all protons have identical values and the signal decay is single exponential [16].

In T_1(H) experiment, the resonance intensities of all the

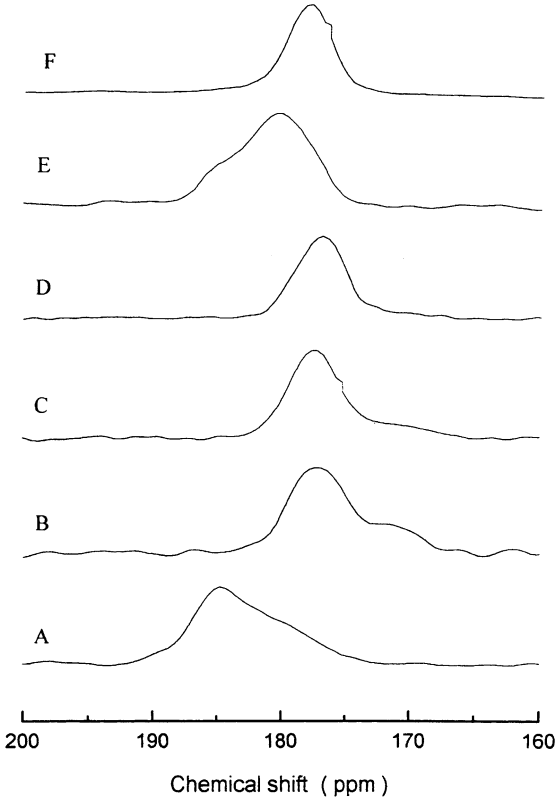

Fig. 8. Logarithmic plot of resonance intensity (at 33 ppm) versus delay time to measure T_1(H). (●) Pure PVP; (□) PAA/PVP blend (1/1); (△) PAA/PVP complex (1/1).

samples were obtained with a series of different delay times based on the inversion recovery mode. The intensity of the resonance carbons can be described by the following exponential model,

$$\ln\left[\frac{(M_e - M_\tau)}{(2M_e)}\right] = \frac{-\tau}{T_1(H)} \quad (2)$$

Fig. 8 shows the logarithmic plot of ^{13}C resonance intensity M_τ versus delay time τ for the selected carbon (33 ppm) of pure PVP, PAA/PVP blend (1/1), and complex. It is found that the fitting of the experiment data with the single exponential decay function is quite well at the entire selected delay time range. The same results were obtained for all the blends and the complex. The T_1(H) values for all

Table 5
The mean value of proton relaxation times in the laboratory frame, $\overline{T_1(H)}$, for PAA/PVP system and the standard deviation σT_1(H)

	Sample	wt/wt	mol/mol	$\overline{T_1(H)}$ (s)	σT_1(H)
	PAA	100/0		2.59	0.01
PAA/PVP	Blend	60/40	2/1	1.77	0.07
PAA/PVP	Blend	40/60	1/1	1.79	0.07
PAA/PVP	Blend	22/78	1/2	2.01	0.12
	PVP	0/100		1.83	0.03
PAA/PVP	Complex	49/51	1.48/1	2.36	0.15

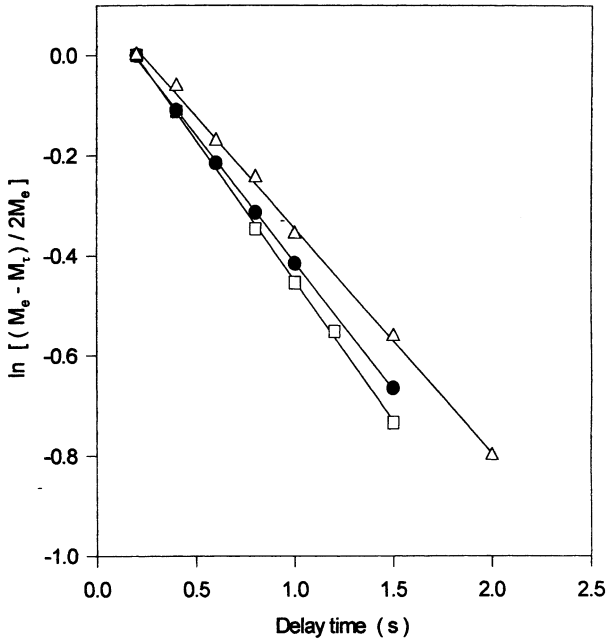

Fig. 9. Logarithmic plot of resonance intensity (at 33 ppm) versus delay time to measure $T_{1\rho}$(H). (●) Pure PVP; (□) PAA/PVP blend (1/1); (△) PAA/PVP complex (1/1).

resonance carbons of all the samples can be obtained as the reciprocal of the slope from the plot of $\ln[(M_e - M_\tau)/(2M_e)]$ versus τ. The mean value of T_1(H)s for each sample was calculated. The calculated mean values of T_1(H)s and the standard deviation are presented in Table 5. It is seen, from Table 5, that the standard deviation in both blends and complex is negligibly small. This indicates that the spin-diffusion among all protons in the blends and the complex can average out the whole relaxation process and hence the domain size of these samples is smaller than the spin-diffusion path length within the time frame of T_1(H). From the obtained value of T_1(H) and using the equation of $L = [6DT_1(H)]^{1/2}$ with $D = 10^{-16}$ m^2/s, it is believed that the PAA/PVP blends are intimately mixed on the T_1(H) measurement scale of 320–390 Å.

The miscibility of the blends and complex can be probed at even smaller scale by carrying out the $T_{1\rho}$(H) measurement, in which the relaxation time, $T_{1\rho}$(H), was determined by monitoring the decay in carbon signal intensities as a function of delay time. $T_{1\rho}$(H) value for individual resonance line was obtained from Eq. (3) by plotting (M_τ/M_0) versus τ.

$$\ln\left(\frac{M_\tau}{M_0}\right) = \frac{-\tau}{T_{1\rho}(H)} \quad (3)$$

All the resonance peaks show a single-exponential decay and the logarithmic plot of ^{13}C resonance intensity M_τ versus delay time τ for the selected carbon (33 ppm) of pure PVP, PAA/PVP blend (1/1), and complex and their linear relationship is shown in Fig. 9. Furthermore, it can

Table 6
The mean value of proton relaxation times in the rotating frame, $\overline{T_{1\rho}(H)}$, for PAA/PVP system and the standard deviation $\sigma T_{1\rho}(H)$

	Sample	wt/wt	mol/mol	$\overline{T_{1\rho}(H)}$ (ms)	$\sigma T_{1\rho}(H)$
	PAA	100/0		6.36	0.01
PAA/PVP	Blend	60/40	2/1	9.34	0.28
PAA/PVP	Blend	40/60	1/1	9.06	0.23
PAA/PVP	Blend	22/78	1/2	9.45	0.52
+ −	PVP	0/100		15.21	0.43
PAA/PVP	Complex	49/51	1.48/1	5.46	0.22

be seen from Table 6 that the standard deviation can be ignored and the $T_{1\rho}(H)$ values obtained for each sample can be considered to be the same. All these imply that all the blends and the complex are intimately mixed on the $T_{1\rho}(H)$ measurement scale. The homogeneity is believed down to the scale of ~20 Å for the blends and ~15 Å for the complex.

In ^{13}C CP/MAS/DD solid state NMR spectra, a resonance line can be observed at 172.9 ppm for the carbonyl carbon of PVP if it is in a non- or weak hydrogen bonded state; otherwise, a resonance line can be observed at 178.8 ppm if it is in strong hydrogen bonded state because the formation of strong hydrogen bonding induces a downfield shift of the carbonyl carbon of PVP [2,12]. The association of PAA and PVP leads to the chemical shift of both the carboxylic carbon resonance of PAA and the amide carbonyl carbon resonance of PVP, resulting in too small difference between the chemical shifts of the two peaks to be resolved. Therefore, only one resonance peak of the carbonyl carbon can be found for the blends and the complex. The carbonyl carbon resonance for the complex (179 ppm) is at the midway between those of the pure components (PAA at 183 ppm and PVP at 176 ppm), while the carbonyl carbon resonance for the blends (around 177 ppm) lies closer to that of PVP. The greater downfield shift observed for the complex than for the blends suggests that the hydrogen bonding formed in the complex is stronger than in the blends.

From the $T_{1\rho}(H)$ measurement, the $T_{1\rho}(H)$ values of the blends lie between those of PAA and PVP, but the $T_{1\rho}(H)$ value of the complex is smaller than those of the two component polymers. The mean $T_{1\rho}(H)$ value of the complex is about half of that of the blends, which indicates that the scale of homogeneity for the complex is even smaller and is calculated to be ~15 Å. The shorter $T_{1\rho}(H)$ relaxation time that the complex attained reflects the rigid nature of the complex.

4. Conclusion

Due to the strong hydrogen bonding interaction between PAA and PVP, both miscible blends and complex can be made. The strong hydrogen bonding is supported by the significant chemical shifts in the FTIR and solid NMR spectra. The chemical shift for FTIR is 24 cm^{-1} and that for solid NMR is 6 ppm. The major structural difference between the PAA/PVP blends and the complex is that the miscible blends can be formed at any molar ratio, whereas the molar ratio for the PAA/PVP complex is always 1.5:1. This ratio may reflect the maximum of hydrogen bonding between the carbonyl and hydroxyl pairs in the two polymers. As a result, more intimate association between the two polymers exists in the polymer complex than in the blends that is supported by the higher T_g and T_d of the complex than those of the blends. The blends are soluble and the complex is insoluble. Such insoluble property might be used in the encapsulation applications that are processed in water solution.

Acknowledgements

Research grant RGC HKUST 6120/99P is greatly acknowledged for supporting this research.

References

[1] Wang H, Li W, Lu Y, Wang Z, Zhong W. J Appl Polym Sci 1996;61:2221.
[2] Tsuchida E, Abe K. Advances in polymer science, vol. 45. Berlin: Springer, 1982.
[3] Moharram MA, Balloomal LS, El-Gendy HM. J Appl Polym Sci 1996;59:987.
[4] Bailey Jr. FE, Lundberg RD, Callard W. J Polym Sci, Part A 1964;2:845.
[5] Utracki LA. Polymer alloy and blends. Munich: Hanser Publishers, 1989.
[6] Chang M, Myerson S, Kwei TK. J Appl Polym Sci 1997;66:279.
[7] Dong J, Ozaki Y, Nakashima K. Macromolecules 1997;30:1111.
[8] Chalapathi VV, Ramiah KV. Curr Sci 1968;16:453.
[9] Zhang X, Takegoshi K, Hikichi K. Macromolecules 1992;25:2336.
[10] Zhang X, Takegoshi K, Hikichi K. Polymer 1992;33:712.
[11] Bovey FA. High-resolution NMR of macromolecules. New York: Academic Press, 1972.
[12] Tonelli AE, Schilling FC. Acc Chem Res 1981;14:233.
[13] Qin C, Priesm ATN, Belifore LA. Polym Commun 1990;31:177.
[14] Miyoshi T, Takegoshi K, Hikichi K. Polymer 1997;38:2315.
[15] Mathias LJ. Solid state NMR of polymers. New York: Plenum Press, 1988.
[16] Lau C, Zheng S, Zhong Z, Mi Y. Macromolecules 1998;31:7291.